The 2013 World Congress on
Advances in Structural Engineering and Mechanics (ASEM13)
Jeju, Korea, September 8-12, 2013

Influence of masonry infills in torsional irregular RC buildings Part 1: Modeling of infills

Theodoros Fotakopoulos[1)], Georgios Mousafeiropoulos[2)], *Marina L. Moretti[3)] and Triantafyllos K. Makarios[4)]

[1), 2), 3)] *Department of Civil Engineering, UTH, Volos 38334, Greece*
[4)] *Department of Civil Engineering, AUTH, Thessaloniki, Greece*
[3)] marmor@uth.gr

ABSTRACT

Masonry infill walls increase considerably the lateral resistance of reinforced concrete buildings, especially in case of a mainly frame structural system. In the design of new structures the contribution of masonry infills is not considered due to the inherent uncertainties of their behavior. However, in case of assessment of the capacity of existing structures to resist future earthquakes the contribution of masonry infills may not be neglected. The masonry infills constitute a significant resource of lateral resistance, the omission of which may be crucial for the capacity of a building for a given seismic performance level.

Although a lot of research has taken place for the modeling of masonry infills, there is still no well accepted method concerning the subject. In the present work the diagonal compressive strut has been applied, which is the macro-model most often used for the simulation of infills. In order to choose the most appropriate parameters, three different strut models have been examined (single-strut, double- and the triple-strut model) to predict the experimental behavior of three different masonry infilled frames from the literature. The different modes of failure of the composite infilled frame are also discussed.

The single-strut model was finally adopted since it led to closer predictions of displacements in the linear analysis, and of force-displacement curves in non-linear static analysis compared to the ones observed in the test. The capacity of the strut was determined not only by the strut resistance in compression but also by considering the shear resistance of the infilled frame depending on the possible failure mechanisms.

1. INTRODUCTION

In the design on new RC buildings the contribution of the masonry infills is not taken into account for a number of factors: Mainly for safety reasons since masonry walls

[1), 2)] Graduate Student
[3)] Assistant Professor, Ph.D.
[4)] Lecturer, Ph.D.

when subjected to cyclic lateral loading exhibit brittle behavior with significant response degradation (Paulay and Priestley 1992) and their contribution to resisting earthquake forces diminishes. For the simulation of infill walls either micro-models are used (finite element approach) or simplified macro-models depicting the structural global behavior of the infilled frame. The most broadly accepted theoretical approach of the latter category is the diagonal strut model with differentiations regarding the strut width and the number and the position of the struts.

In this work the use of several simplified strut models is discussed in relation to the capacity of each model to simulate the response of selected tested infilled RC frames. Another significant and rather complex matter is the definition of failure of an infilled frame. All possible failure mechanisms should be considered so as to estimate the resistance to be used for the simulation and the assessment of the behavior of an infilled frame.

2. MODES OF FAILURE OF MASONRY INFILLED RC FRAMES

The various modes of failure of masonry infilled frames have been extensively investigated both experimentally and analytically. In this work the possible failure mechanisms proposed by Shing and Mehrabi (2002) and presented by Kyriakides (2011) have been considered (Fig. 1).

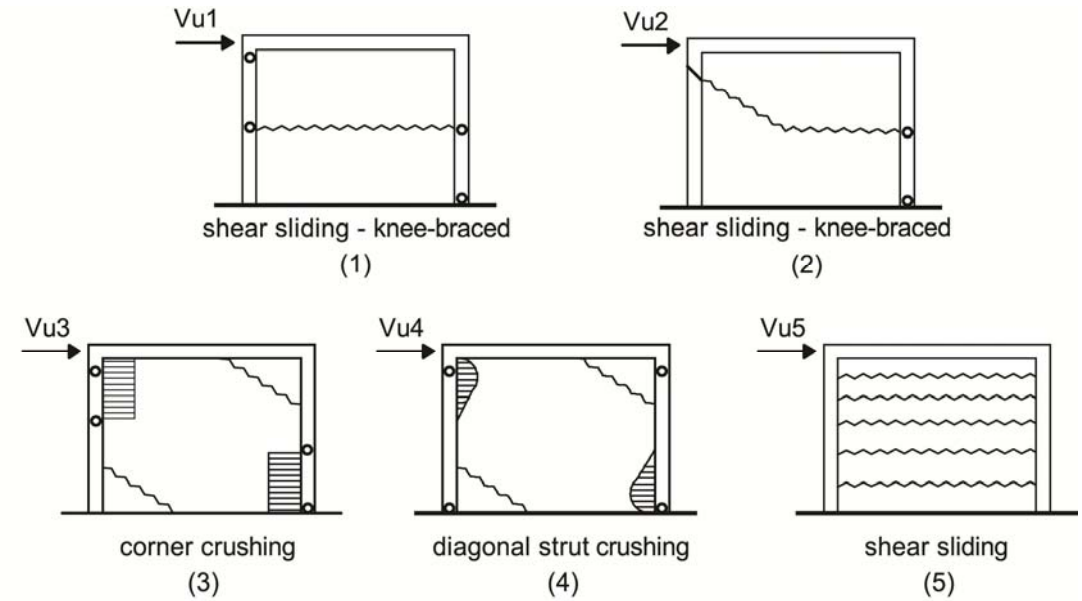

Fig. 1 Suggested modes of failure of a masonry infilled RC frame (Shing and Mehrabi, 2002)

The resistance of each mechanism is calculated by considering the individual load bearing mechanisms activated in every case. The resistance of the failure modes (1), (2) and (5) is calculated by formulas suggested by Mehrabi et al (1994), while the resistance of cases (3) and (4) is calculated with the application of plastic analysis as

suggested by Liauw and Kwan (1985). The lower value of the calculated resistances is supposed to characterize the decisive mode of failure of the infilled frame.

3. STRUT MODELS FOR INFILL WALLS IN RC FRAMES

The “diagonal strut” has been chosen for modeling the infills in this work due to its simplicity in application for design purposes. A diagonal strut model is a linear element connected through pins to the joints of the frame, capable of resisting only compressive forces. The thickness of the strut is assumed equal to the thickness of the infill panel. The characteristics of the strut are similar to those of the infill.

In current codes the strut width, w, is calculated either as a percentage of the length of the diagonal of the infill (Holmes 1961, KAN.EPE 2012) or by taking into account the relative stiffness of the infill and the columns of the frame as well as the length of the infill diagonal (Fema 356, 2000). The latter approach described by equations (1) and (2) was considered as most appropriate and will be used in this work since it illustrates the enhanced activation of the infill in case of stiffer frame columns.

$$\lambda = \sqrt[4]{\frac{(E_m t_{inf} \sin 2\theta)}{4 E_f I_{col} h_{inf}}} \quad (1)$$

$$w = 0.175 \, (\lambda \, h_{col})^{-0.4} \, r_{inf} \quad (2)$$

where E_m, t_{inf}, and h_{inf} are the Young’s modulus of elasticity, thickness and height of infill, E_f and I_{col} are the Young’s modulus of elasticity and moment of inertia of the columns, while θ is the angle whose tangent is the infill’s height-to-length aspect ratio.

Use of more-fold strut models, instead of a single strut, have been also suggested mainly with the intention of depicting the complicated behavior of the infilled frame (Thiruvengadam 1985, Chrysostomou et al 2002). It has been decided to examine three different strut models for the simulation of infill walls: single-strut, 2-strut and 3-strut models. All three models have been applied to three tested masonry infilled frames from the literature. The analytical predictions are compared to the experimental data and the results are discussed in relation to the adequacy of each model to better estimate the maximum displacement and the resistance of the infilled frames tested.

When a single-strut model is used to substitute the infill, in which the strut connects the main frame diagonal subjected to compression, the strut width, w, is calculated from Eqs. (1) and (2).

In case of a 2-strut model each strut width is calculated according to Eqs. (1) and (2). The geometrical position of the struts (Fig. 2) is calculated using the following equations (Fiore et al, 2012):

For strut 1 in the first storey

$$\frac{d_1}{H} = 0.10834\left(\frac{L}{H}\right)^{-1} + 0.0073141\left(\frac{L}{H}\right)^{2} \quad (3a)$$

$$\frac{b_1}{L} = 0.48689\left(\frac{L}{H}\right)^{-2} + 0.16302\left(\frac{L}{H}\right)^{-0.5} \quad (3b)$$

For strut 1 in the upper storeys:

$$\frac{d_1}{H} = 0.11609\left(\frac{L}{H}\right)^{-1} + 0.0061624\left(\frac{L}{H}\right)^{2} \tag{4a}$$

$$\frac{b_1}{L} = 0.56509\left(\frac{L}{H}\right)^{-1} + 0.1287\left(\frac{L}{H}\right)^{0.5} \tag{4b}$$

For strut 2 in the first storey

$$\frac{d_2}{H} = 0.157621\left(\frac{L}{H}\right)^{-1} + 0.084484\left(\frac{L}{H}\right)^{0.5} \tag{5a}$$

$$\frac{b_2}{H} = 0.408621\left(\frac{L}{H}\right)^{-0.5} + 0.44431\left(\frac{L}{H}\right)^{0.5} \tag{5b}$$

For strut 2 in the upper storeys

$$\frac{d_2}{H} = 0.1025\left(\frac{L}{H}\right)^{-0.5} + 0.046736\left(\frac{L}{H}\right)^{0.5} e^{(L/H)^{-0.5}} \tag{6a}$$

$$\frac{b_2}{H} = 0.312751\left(\frac{L}{H}\right)^{-1.5} + 0.467931\left(\frac{L}{H}\right)^{0.5} \tag{6b}$$

In the 3-strut model one strut was placed along the diagonal under compression ("windward" diagonal) and the other two struts were placed at both sides of the main diagonal at distances l_{ceff} and l_{beff} from the corner joints calculated from Eqs (7a), (7b), (8a) and (8b) (FEMA 356, 2000).

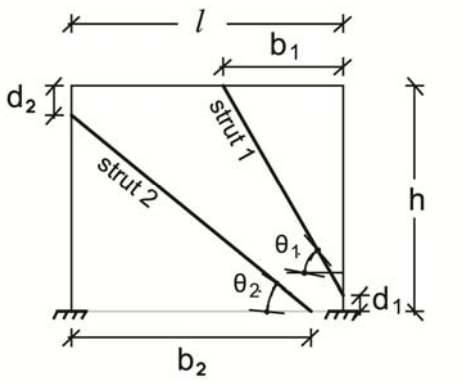

Fig. 2 Position of struts in the 2-strut model for masonry infills (Fiore et al. 2012)

$$l_{ceff} = \frac{w}{\cos\theta_c} \tag{7a}$$

where

$$\tan\theta_c = \frac{(h_{inf} - \frac{w}{\cos\theta_c})}{L_{inf}} \tag{7b}$$

$$l_{beff} = \frac{w}{\sin\theta_b} \tag{8a}$$

where

$$\tan\theta_b = \frac{h_{inf}}{L_{inf} - \frac{w}{\sin\theta_b}} \tag{8b}$$

The strut width, w, is calculated by means of Eqs. (1) and (2) and it is shared by the three struts as follows: 50% w in the strut in the middle and 25% w in the two other struts.

4. ASSESSMENT OF STRUT MODELS IN TESTED INFILLED FRAMES

The three different strut models presented above were applied in a simple engineering model with the intention to reproduce the behavior of 3 one-bay RC frames with masonry infills, fixed at their base, that have been tested under horizontal cyclic loading: a 1-storey flexible frame (Kakaletsis and Karayannis, 2009), a 1-storey stiff frame (Blackard et al., 2009), and a 2-storey frame (Baran and Sevil, 2010).
The modulus of elasticity E_w of the infill along the inclined struts at an angle θ to the horizontal is calculated by Eq. (9) (El-Dakhakhni et al, 2003). The moduli of elasticity Einfill-0 and Enifill-90 of the masonry infill, at directions perpendicular and parallel to the holes of the masonry block, respectively, were assumed to be equal when relevant experimental data were not provided by the authors. In the absence of specific data the shear modulus of the masonry infill was assumed $G=0.4E_{infill\text{-}90}$ (Fema 356, 2000). Poisson's ratio was assumed to be v =0.15 (Mohamad et al, 2006).

$$E_{infill\_\theta} = \frac{1}{\frac{1}{E_{infill\_0}}\cos^4\theta + [-\frac{2\nu}{E_{infill\_0}} + \frac{1}{G}]\cos^2\theta\cdot\sin^2\theta + \frac{1}{E_{infill\_90}}\sin^4\theta} \tag{9}$$

The effective flexural stiffness, K_{eff}, of the frame members in the analyses was calculated as proposed in Eurocode 8 part 3 (CEN 2005) in paragraph A3.2.4 (5), i.e. the mean value of $M_yL_v/3\theta_y$ at the two ends of the elements, where M_y is the yield

moment, L_v is the shear span taken to be equal to half the element length, and θ_y is the chord rotation at yielding, calculated by Eq. (10) also found in Eurocode 8 part 3 (CEN 2005).

$$\theta_y = \varphi_y \frac{L_v + a_v z}{3} + 0,00135(1+1,5\frac{h}{L_v}) + \frac{\varepsilon_y}{d-d'}\frac{d_b f_{yk}}{6\sqrt{f_{ck}}} \quad (10)$$

where

φ_y yield curvature of the end section
α_v = 1 if shear cracking precedes flexural failure
z length of the internal lever arm, taken equal to d-d'
f_{yk}, f_{ck} characteristic values of yield stress and the concrete strength respectively
d, d' depths to the tension and compression reinforcement, respectively

The characteristics of the tested frames that have been analyzed are as follows:

(a) One-storey flexible frame tested by Kakaletsis and Karayannis (2009), scale 1/3, with total dimensions: L x h = 1.50 m x 1.05 m, where L, h are the total length and height of the frame, respectively.

Characteristics of the infill wall: thickness t=0.06 m, modulus of elasticity E_w= 628.44 MPa.

The characteristics of the frame members are as follows: Columns: cross-section 0.15 m x 0.15 m, longitudinal reinforcement 8 bars Φ5.6 mm diameter (f_{sy} = 390.47 MPa), and stirrups Φ3@50mm (f_{wy} = 212.20 MPa). Beam: cross-section b x h = 0.10 m x 0.20 m, tensile and compressive longitudinal reinforcement 3Φ5.6 mm (f_{sy} = 390.47 MPa), and 2Φ5.6 mm (f_{sy} = 390.47 MPa), respectively and stirrups Φ3@60mm (f_{wy} = 212.20 MPa). Compressive cylinder strength of concrete: f_{cc}= 28.51 MPa.

Axial compressive load at each column, N= 50 kN.

(b) One-storey stiff frame tested in Colorado by Blackard et al, scale 2/3, with total dimensions: L x h = 4.49 m x 2.64 m, where L, h are the total length and height of the frame, respectively.

Characteristics of the infill wall: thickness t=0.10 m, modulus of elasticity E_w= 9196.12 MPa.

The characteristics of the frame members are as follows: Columns: cross-section 0.279 m x 0.279 m, longitudinal reinforcement 4 bars Φ9.52 mm diameter and 4 bars Φ12.7 diameter (f_{sy} = 20.7 MPa), and stirrups Φ6.35@150mm (f_{wy} = 455 MPa). Beam: cross-section b x h = 0.279 m x 0.368 m, tensile and compressive longitudinal reinforcement 2Φ19.1 mm (f_{sy}= 455 MPa) and stirrups Φ6.35@150mm (f_{wy} = 455 MPa). Compressive cylinder strength of concrete: f_{cc}= 20.7 MPa.

Axial compressive load at each column, N = 156 kN.

(c) Two-storey frame tested by Baran and Sevil (2010), scale 1/3, with total dimensions: L x h = 1.50 m x 1.80 m, where L, h are the total length and height of the frame, respectively (Fig. 4).

Characteristics of the infill wall: thickness t = 0.09 m, modulus of elasticity Ew =

1802.42 MPa.

The characteristics of the frame members are as follows: Columns: cross-section 0.10 m x 0.15 m, longitudinal reinforcement 4 bars Φ8 mm diameter (f_{sy} = 500 MPa), and stirrups Φ4@100mm (f_{wy} = 500 MPa). Beam: cross-section b x h = 0.15 m x 0.15 m, tensile and compressive longitudinal reinforcement 3Φ8 mm (f_{sy}= 500 MPa) and stirrups Φ4@100mm (f_{wy} = 500 MPa). Compressive cylinder strength of concrete: f_{cc}= 12 MPa.

Axial compressive load at each column, N = 58.85 kN.

Frames with the same dimensions, materials and reinforcement as the ones tested were modeled through SAP2000 for the three different strut models. The results have been used to determine the most appropriate strut model to use for simulating the behavior of the infills in such a way that the analysis model reproduces as close as possible the experimental behavior of the infilled frame.

Initially the frames were loaded to the maximum experimental loads P_{max}. The top horizontal frame displacements, δ, calculated by the model are shown in Tables 1 to 3. It is evident that the 2-strut model overestimates in general considerably the displacement at maximum load. Therefore in the following procedures only the 1- and the 3-strut models were used.

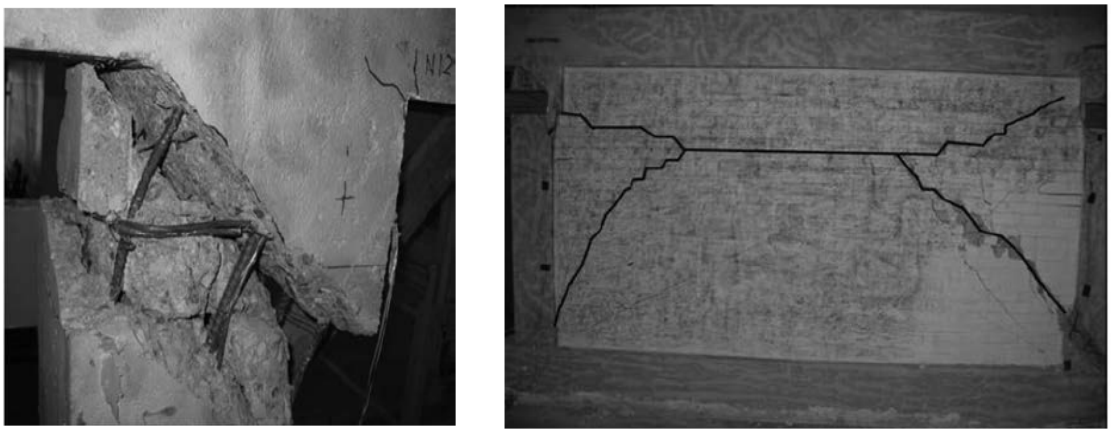

(a) failure of infill (b) shear failure of frame column

Fig. 3 Mode of failure of the stiff frame tested by Blackard et al

The shear resistances V_{u1} to V_{u5} for the five possible failure mechanisms of an infilled frame shown in Figure 1 have been calculated according to Shing and Mehrabi (2002) and are also displayed in Tables 1 to 3. In Figures 3 and 4 are shown the actual modes of failure of the stiff and the 2-storey frame, respectively.

Failure modes (1) and (4) have been chosen as the most representative and they will be considered to calculate the shear resistance of the infilled frames: On one hand they include the most probable types of failure, and on the other hand the calculated respective shear resistances V_u may be used as a safe limit to estimate the shear resistance of an infilled frame.

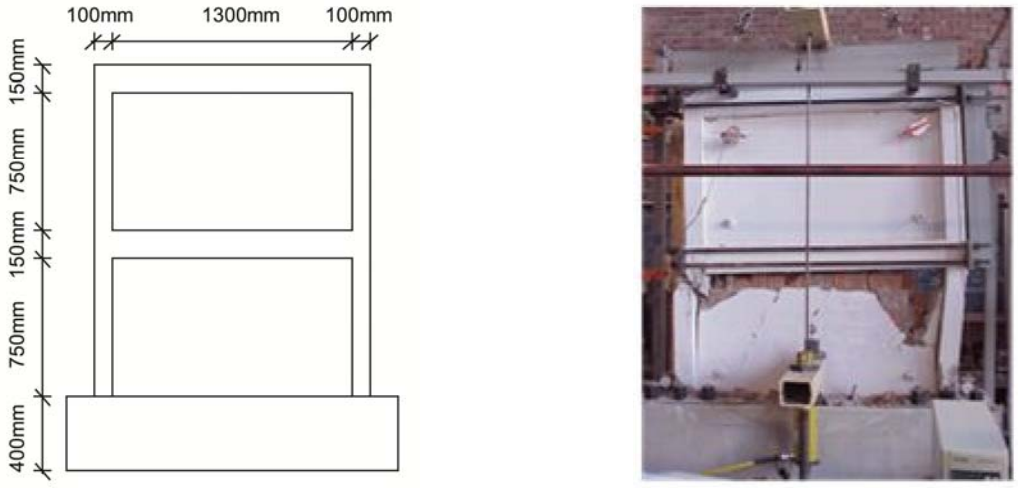

(a) Dimensions of specimen (b) Mode of failure

Fig. 4 Two-storey frame tested by Baran and Sevil (2010)

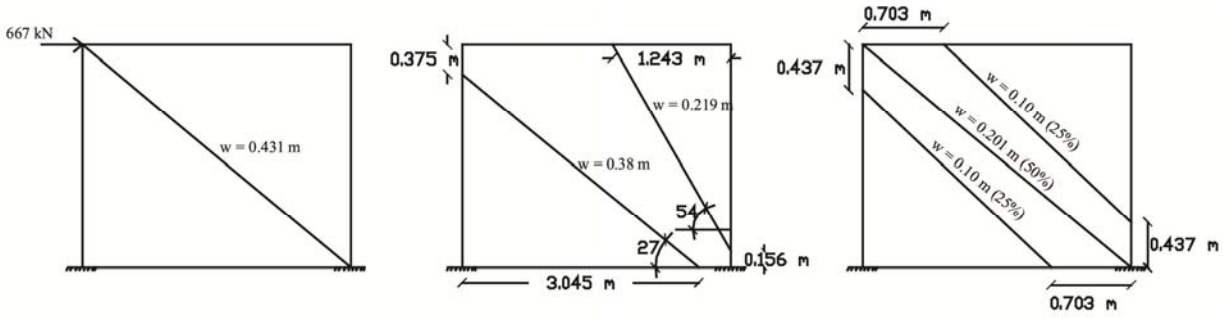

Fig. 5 Strut models considered for the stiff frame (Blackard et al)

Table 1 One-storey flexible infilled frame (Kakaletsis et al, 2009): Failure loads, V_u and storey frame displacements, δ, from linear analysis for $P=P_{max}=80$ kN

EXPERIMENTAL RESULTS			SINGLE STRUT		DOUBLE STRUT		TRIPLE STRUT	
Pmax:	80	kN	39,63	kN	41,57	kN	41,65	kN
Displacement at top of frame:	0,012	m	0,0144	m	0,0129	m	0,015	m
Sliding of infill with plastic hinges at mid-height of the columns			V_{u1} = 64,42	kN	V_{u1} = 69,31	kN	V_{u1} = 69,08	kN
Sliding of infill with shear failure in one column and plastic hinge at mid-height of the other (or shear failure)			V_{u2} = 53,89	kN	V_{u2} = 55,83	kN	V_{u2} = 55,92	kN
Brittle failure of the infill corners and plastic hinge in column at a distance y			V_{u3} = 100,95	kN	V_{u3} = 103,86	kN	V_{u3} = 103,9	kN
Compressive failure of infill at the corners and plastic hinges at the ends of columns			V_{u4} = 74,08	kN	V_{u4} = 76,02	kN	V_{u4} = 76,11	kN
Sliding of infill with plastic hinges at ends of columns			V_{u5} = 39,63	kN	V_{u5} = 41,57	kN	V_{u5} = 41,65	kN

Table 2 One-storey stiff infilled frame (Blackard et al): Failure loads, V_u and storey frame displacements, δ, from linear analysis for $P=P_{max}$ =667 kN

EXPERIMENTAL RESULTS			SINGLE STRUT		DOUBLE STRUT		TRIPLE STRUT	
Pmax:	667	kN	252,45	kN	278,09	kN	263,9	kN
Displacement at top of frame:	0,0054	m	0,0079	m	0,0135	m	0,009	m
Sliding of infill with plastic hinges at mid-height of the columns			V_{u1} = 320,6	kN	V_{u1} = 357,5	kN	V_{u1} = 332,1	kN
Sliding of infill with shear failure in one column and plastic hinge at mid-height of the other (or shear failure)			V_{u2} = 277,5	kN	V_{u2} = 303,1	kN	V_{u2} = 288,9	kN
Brittle failure of the infill corners and plastic hinge in column at a distance y			V_{u3} = 604,4	kN	V_{u3} = 681,6	kN	V_{u3} = 640,1	kN
Compressive failure of infill at the corners and plastic hinges at the ends of columns			V_{u4} = 439,5	kN	V_{u4} = 464,9	kN	V_{u4} = 450,9	kN
Sliding of infill with plastic hinges at ends of columns			V_{u5} = 252,4	kN	V_{u5} = 278,1	kN	V_{u5} = 263,9	kN

Table 3 Two-storey infilled frame (Baran and Sevil, 2010): Failure loads, V_u and storey frame displacements, δ, from linear analysis for $P=P_{max}$ = 74.19 kN

	EXPERIMENTAL RESULTS			SINGLE STRUT		DOUBLE STRUT		TRIPLE STRUT	
First storey	Pmax:	74,19	kN	48,50	kN	50,77	kN	48,50	kN
	Top frame displ.:	0.0039	m	0,0053	m	0,0063	m	0,0059	m
	Sliding of infill with plastic hinges at mid-height of the columns			V_{u1} = 62,96	kN	V_{u1} = 68,76	kN	V_{u1} = 62,96	kN
	Sliding of infill with shear failure in one column and plastic hinge at mid-height of the other (or shear failure)			V_{u2} = 48,88	kN	V_{u2} = 51,15	kN	V_{u2} = 48,88	kN
	Brittle failure of the infill corners and plastic hinge in column at a distance y			V_{u3} = 69,53	kN	V_{u3} = 73,89	kN	V_{u3} = 69,53	kN
	Compressive failure of infill at the corners and plastic hinges at the ends of columns			V_{u4} = 53,06	kN	V_{u4} = 55,93	kN	V_{u4} = 53,06	kN
	Sliding of infill with plastic hinges at ends of columns			V_{u5} = 48,50	kN	V_{u5} = 50,77	kN	V_{u5} = 48,50	kN
	EXPERIMENTAL RESULTS			SINGLE STRUT		DOUBLE STRUT		TRIPLE STRUT	
Second storey	Pmax:	46,49	kN	48,50	kN	54,99	kN	54,93	kN
	Top frame displ.:	0,0062	m	0,0053	m	0,0105	m	0,0099	m
	Sliding of infill with plastic hinges at mid-height of the columns			V_{u1} = 74,39	kN	V_{u1} = 74,59	kN	V_{u1} = 74,39	kN

Second storey	Sliding of infill with shear failure in one column and plastic hinge at mid-height of the other (or shear failure)	V_{u2} = 55,31 kN	V_{u2} = 55,37 kN	V_{u2} = 55,31 kN
	Brittle failure of the infill corners and plastic hinge in column at a distance y	V_{u3} = 81,27 kN	V_{u3} = 81,37 kN	V_{u3} = 81,27 kN
	Compressive failure of infill at the corners and plastic hinges at the ends of columns	V_{u4} = 59,49 kN	V_{u4} = 60,15 kN	V_{u4} = 59,49 kN
	Sliding of infill with plastic hinges at ends of columns	V_{u5} = 54,93 kN	V_{u5} = 54,99 kN	V_{u5} = 54,93 kN

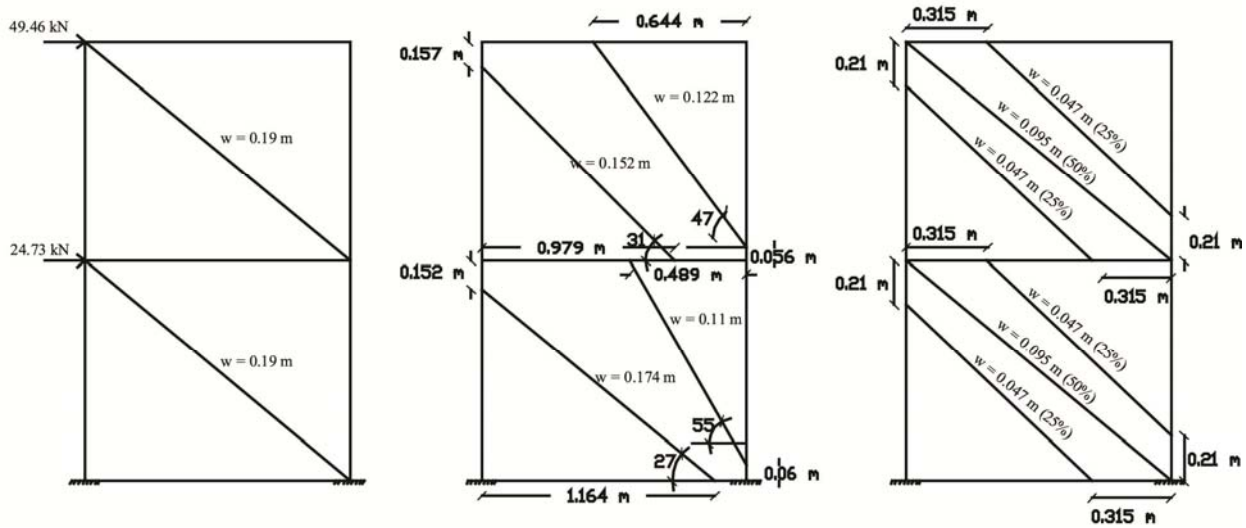

Fig. 6 Strut models considered for the frame of Baran and Sevil (2010)

For the simulation of the force-displacement curve of the tested frames considered a pushover analysis was performed and the P-δ curves were compared to the experimental ones. Only the 1-strut and 3-strut models were used for the infills, since the 2-strut model was considered inadequate, as previously mentioned.

The non-linear stress-strain (σ-ε) relationship of the infills used is shown in Fig. 7a (KAN.EPE, draft 2006). After several trials it was found that best fit of the pushover curve to the experimental P-δ curve was achieved for the average values: ε_y = 0.00125 and ε_u = 0.00275 and these values have been adopted. The effective stiffness that was assumed for the link element used to simulate the strut in SAP2000 is

$$K_{eff} = \frac{E_{\inf,\theta} \cdot w \cdot t}{r_{\inf}} \tag{11}$$

where $E_{inf,\theta}$ is the modulus of elasticity of the infill along angle θ
w is the strut width

t and r_{inf} are the thickness and the length of the diagonal, respectively

The typical moment-chord rotation relationship (M-θ) assumed for the plastic hinges of the frame members is shown in Fig. 7b. The values θ_y and θ_u are calculated according to Eqs. (10) and (12) of Eurocode 8 part 3 (CEN 2005). Residual strength of 20%M_y was assumed (Makarios, 2013).

$$\theta_{um} = \frac{1}{\gamma_{el}} 0.016(0.3^{\nu})[\frac{\max(0.01;\omega')}{\max(0.01;\omega)} f_c]^{0.225} (\frac{L_v}{h})^{0.35} 25^{(a\rho_{sx}\frac{f_{yw}}{f_c})} \quad (12)$$

where

γ_{el} = 1.5 for primary seismic elements

h is the depth of cross-section

$v = N / bhf_c$ (b width of compression zone, N axial force positive for compression)

ω', ω are the mechanical longitudinal reinforcement ratios of the tension and compression reinforcement, respectively.

f_c, f_{yw} are the concrete compressive strength (MPa) and the stirrup yield strength (MPa).

$\rho_{sx} = A_{sx}/b_w s_h$ is the ratio of transverse steel parallel to the direction x of loading (s_h = stirrup spacing)

α is the confinement effective factor (Eurocode 8 part 1, CEN 2004b).

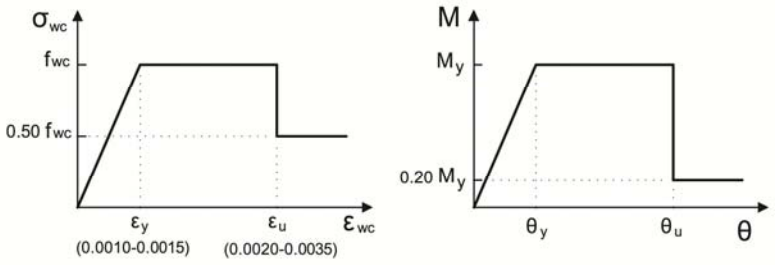

(a) (b)

Fig. 7 (a) Non-linear diagram σ-ε for non-reinforced masonry under compression; (b) Moment-chord rotation diagram for flexural failure of frame members

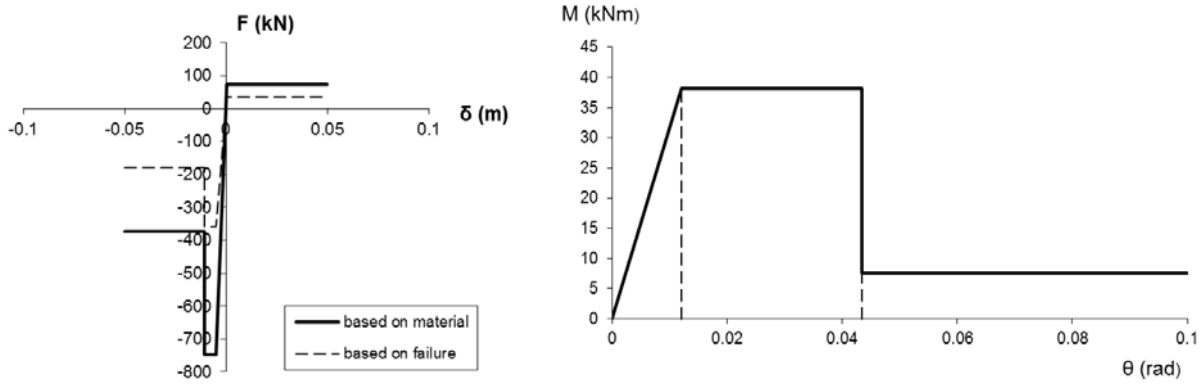

Masonry characteristics frame plastic hinges characteristics

Fig. 8 Material characteristics in the one-storey stiff frame model

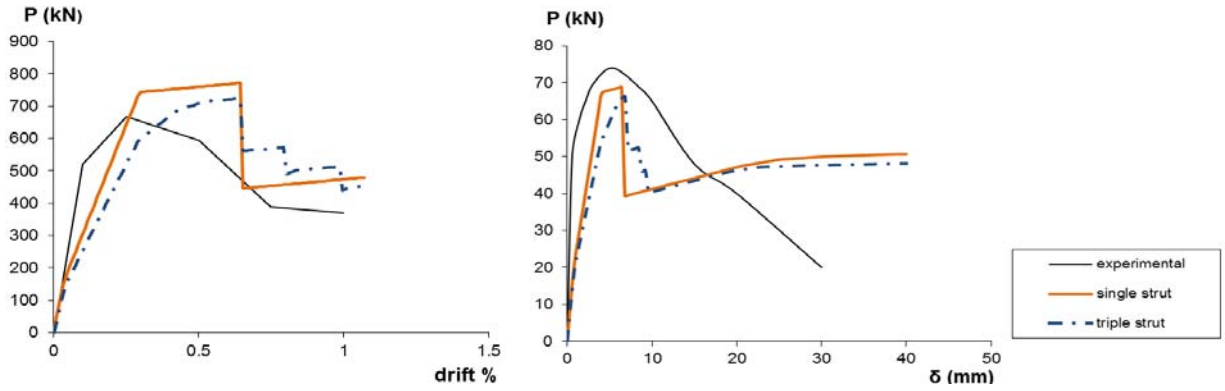

one-storey stiff frame two-storey frame

Fig. 9 Pushover curves from the single- and triple-strut infill model, compared to the experimental envelope of load-displacement hysteresis loops

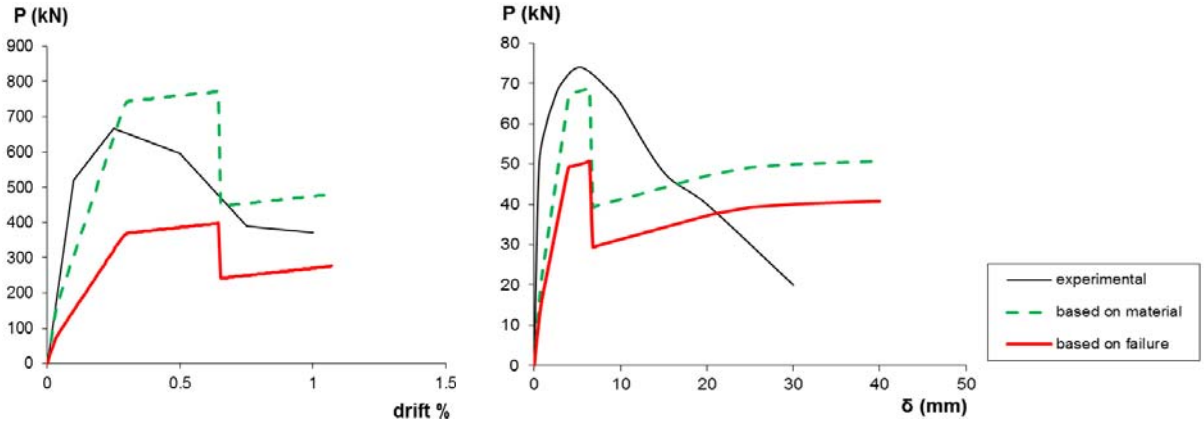

one-storey stiff frame two-storey frame

Fig. 10 Pushover curves with single-strut infill model, for strut characteristic calculated according to material properties and to shear resistance of the infilled frame

The single-strut model describes better the behavior of the tested models than the 3-strut model, as shown from the comparison of the respective pushover curves to the experimental P-δ diagram (Fig. 9). In Fig. 10 are shown the pushover curves for the two frames that were modeled through the single-strut model: The F-δ diagram of the infill was calculated both by the material properties of the masonry infill and by the force along the strut that corresponds to the shear resistance of the frame, as calculated by Shing and Meharbi (2002) for the minimum between the values V_{u2} and V_{u4}, as described previously. The simulation of the infill according to the calculated shear resistance of the infilled frame produces the best approximation.

5. CONCLUSIONS

In this work it has been attempted to reproduce the experimental behavior of three tested frames found in the literature through various strut model. It has been found that

the single strut model leads to a better approximation of the actual force-displacement diagrams of the specimens considered. Still better approximation is obtained if the strength of the infill assumed for the strut model is calculated by taking into account also the expected shear resistance of the infilled frame for the expected modes of failure.

REFERENCES

Blackard B., Willam K., and Mettupalayam S. “Experimental Observations of Masonry Infilled Reinforced Concrete Frames with Openings”, *ACI, SP-265—9, 199-221.*

Baran M. and Sevil T. (2010) “Analytical and experimental studies on infilled RC frames”, *International Journal of the Physical Sciences, Vol. 5(13), 1981-1998.*

Chrysostomou C.Z., Gergely P. and Abel J.F. (2002), “A six-strut model for nonlinear dynamic analysis of steel infilled frames”, *Int. J. Struct. Stab. Dyn., 2(3), 335–353.*

CEN (2004a) European Standard EN1998-1:2004 *Eurocode 8: Design of structures for earthquake resistance - Part 1: General rules, seismic actions and rules for buildings*, European Committee for Standardization, Brussels.

CEN (2004b) European Standard EN1992-1-1:2004 Eurocode 2: *Design of concrete structures - Part 1-1: General rules and rules for buildings*, European Committee for Standardization, Brussels.

CEN (2005) European Standard EN1998-3:2005 Eurocode 8: *Design of structures for earthquake resistance - Part 3: Assessment and retrofitting of buildings*, European Committee for Standardization, Brussels.

El-Dakhakhni W.W, Elgaaly M, Hamid A.A (2003) “Three-Strut Model for Concrete Masonry-Infilled Steel Frames”, *J. Struct. Eng., 177-185.*

Fardis M.N. (2009), *“Seismic design, assessment and retrofitting of concrete buildings”*, Springer.

Fardis M.N., Bousias S.N, Franchioni G. and Panagiotakos T.B. (1999), “Seismic response and design of RC structures with plan-eccentric masonry infills”, *Earthquake Eng. Struct. Dyn. 28: 173-191.*

FEMA 356 (2000). “*Prestandard and commentary for the seismic rehabilitation of buildings*.” Washington DC.

Fiore A., Netti A., Monaco P., *“The influence of masonry infill on the seismic behaviour of RC frame buildings”,* Politecnico di Bari, Dep. of Science of Civil Engineering and Architecture, Via Orabona 4, 70125 Bari, Italy, 2012.

Holmes, H. (1961), “Steel frames with brickwork and concrete infilling”, *Proc. ICE, No. 6501, 473-478.*

KAN.EPE (2012), *“Hellenic code for retrofit of RC buildings.”* Greek Earthquake Planning and Protection Organization (in Greek).

Kakaletsis D.J. and Karayannis C.G. (2009), “Experimental investigation of infilled reinforced concrete frames with openings”, *ACI Structural Journal, 106-S14, 132-141.*

Kyriakides, M.A. (2011), *“Seismic retrofit of unreinforced masonry infills in non-ductile reinforced concrete frames using engineered cementitious composites”*, Dissertation submitted to the Dept. of Civil and Environ. Eng. of Stanford University in partial

fulfillment of requirements for PhD degree.
Liauw, T.C. and Kwan, K.H. (1985), “Unified Plastic Analysis for Infilled Frames”, *ASCE Journal of Structural Engineering, 111(7), pp. 1427-1448*.
Mainstone, R.J. (1971), “On the stiffnesses and strengths of infilled frames.” *Proc. ICE Suppl., Paper No. 7360S, 57-90.*
Makarios, T.K. (2013), “*Modeling of characteristics of inelastic members of RC structures in seismic nonlinear analysis”, Chapter 1, 1-42,* Nova Publishers, New York.
Mehrabi, A.B., Shing, P.B., Schuller, M.P., and Noland, J.L. (1994), *“Performance of Masonry-Infilled R/C Frames under In-Plane Lateral Loads”,* Report No.CU/SR-94-6, Dept. of Civil, Environmental, and Architectural Engineering, University of Colorado, Boulder, CO.
Mohamad G., Lourenco P.B., Roman H.R. (2006), “*Mechanics of hollow concrete block masonry prisms under compression: Review and prospects*”, Dept. of Civil Engineering, Univ. of Minho, CAPES-MEC-UNIVALI UNESC, Azurem, Portugal Civil Engineering Department of Federal University of Santa Catarina, Brazil.
Paulay, T. and Priestley, M.J.N. (1992), *“Seismic design of reinforced concrete and masonry buildings”,* Wiley, New York.
Shing, P.B. and Mehrabi, A.B. (2002), “Behavior and Analysis of Masonry-Infilled Frames”, *Progress in Structural Engineering and Materials, 4(3), pp. 320-331.*
Stafford Smith, B. (1966), “Behavior of the square infilled frames.” *J. Struct. Div. ASCE, 92(1), 381-403.*
Stafford Smith, B. and Carter, C. (1969), “A method of analysis for infilled frames.” *Proc. ICE., Vol. 44, 31-48.*
Thiruvengadam V. (1985), “On the natural frequencies of infilled frames”, *Earthquake Eng. Struct. Dyn., 13(3), 401–419.*